ELSEVIER

Composite Structures 59 (2003) 369–383

COMPOSITE STRUCTURES

www.elsevier.com/locate/compstruct

Minimization of the dynamic response of composite laminated doubly curved shells using design and control optimization

M.E. Fares *, Y.G. Youssif, A.E. Alamir

Department of Mathematics, Faculty of Science, Mansoura University, Mansoura 35516, Egypt

Abstract

A design control optimization approach is used to determine optimal levels of ply thickness, fiber orientation angle and closed-loop control force for composite laminated doubly curved shells. The optimization objective is the minimization of the dynamic response of a shell subject to constraints on the thickness and control energy. A higher-order shell theory is used to formulate the control objective for various cases of boundary conditions. The dynamic response is expressed as the sum of the total elastic energy of the shell and a penalty functional of a closed-loop control force. Comparative examples are presented for symmetric (or anti-symmetric) spherical and cylindrical shells with various cases of boundary conditions. The advantages of the present control optimization over some design and control approaches are examined. The effect of number of layers, aspect ratio and orthotropy ratio on the control process is demonstrated. The discrepancy between optimal results obtained using the classical, first-order and higher-order shell theories is studied.

Keywords: Structures design and control; Closed-loop control force; Optimal layer thickness; Fiber orientation angle; Higher-order shell theory

1. Introduction

An important area of application of fiber composite structures occurs in the field of aerospace engineering and, in particular, in the construction of large space structures. Material tailoring and active control are effective means of improving the performance of these structures because of the adaptability of composite materials to a given design situation. For aerospace structures, weight considerations invariably lead to highly flexible structures with low natural damping. However, serviceability and safety requirements restrict the allowable limits of the dynamic response to external disturbances to specified values. So, optimization is a necessary part of the design process for these structures.

Design optimization of composite laminated structures is concerned with the best use of the tailoring capabilities of fiber-reinforced laminated beams, plates and shells to minimize (or maximize) a given design objective. The vibration damping involves the damping out of the excessive vibrations by means of active structural control. These two subjects were treated in literature separately [1–4], while, in more recent studies, they were treated as an integrated approach for simultaneous design and control of these structures using unified formulation [5–8]. Most recent studies on these subjects may be found in the works [9–14].

Many studies indicate that transverse shear deformation can have significant effect on the global response and, consequently, on the dynamic response of laminated plates and shells made of advanced composite material [15,16]. As a result, the classical theories of laminated plates and shells underpredict the optimum values of the design variables. In addition, the boundary conditions at the edges play an important role in decreasing (or increasing) the dynamic response of laminated composites [17]. However, most of studies related to the design and control optimization of laminated composite plates and shells were carried out based on the classical theories of plates and shells for special cases of boundary conditions, and there exist few papers formulated based on shear deformation theories for various cases of boundary conditions [18,19].

* Corresponding author. Tel.: +20-50-346-781; fax: +20-50-346-254.
E-mail address: sinfac@mum.mans.eun.eg (M.E. Fares).

0263-8223/03/$ - see front matter
PII: S0263-8223(02)00241-6

The current work deals with the minimization of the dynamic response of a composite laminated doubly curved shells using design and control optimization. The present formulation is based on a higher-order shear deformation shell theory with various cases of boundary conditions. The dynamic response of the shell is expressed as the sum of the total energy of the shell and a penalty functional involving closed loop control force. The ply thickness and fiber orientation angle are taken as design variables. Liapunov–Bellman theory is used to obtain solutions for controlled shell deflections and optimal control force. Various examples and numerical results for laminated symmetric (or antisymmetric) cylindrical and spherical shells are given. The effect of boundary conditions, number of layers, anisotropy ratio, aspect ratio, side-to-thickness ratio and radius-to-thickness ratio on the minimization process is illustrated.

2. Geometry of the shell and basic equations

Let (ξ_1, ξ_2, z) denote the orthogonal curvilinear coordinates (or shell coordinates) such that the ξ_1- and ξ_2-curves are lines of curvature on the midsurface $z = 0$, and z-curves are straight lines perpendicular to the surface $z = 0$. For spherical and cylindrical shells, the lines of principal curvature coincide with the coordinate lines. The values of the principal radii of curvature of the middle surface are denoted by R_1 and R_2. In this case, the distance $\mathrm{d}S$ between two points (ξ_1, ξ_2, z) and $(\xi_1 + \mathrm{d}\xi_1, \xi_2 + \mathrm{d}\xi_2, z + \mathrm{d}z)$ is given by

$$(\mathrm{d}S)^2 = L_1^2(\mathrm{d}\xi_1)^2 + L_2^2(\mathrm{d}\xi_2)^2 + L_3^2(\mathrm{d}z)^2,$$

where Lame's coefficients L_1, L_2 and L_3 are related to the surface metrics α_1, α_2 and α_3 by the following relations:

$$L_1 = \alpha_1\left(1 + \frac{z}{R_1}\right), \quad L_2 = \alpha_2\left(1 + \frac{z}{R_2}\right), \quad L_3 = 1. \tag{1}$$

The shell under consideration is composed of a finite number of orthotropic layers N with total constant thickness h. Let z_k and z_{k-1} be the top and bottom z-coordinates of the kth lamina. The present study is based on a higher-order displacement field satisfying the condition that the transverse shear stresses vanish on the top and bottom surfaces of the shell. This displacement field is given by [20]

$$u_1 = \frac{1}{\alpha_1}(L_1 u) + z\psi - \frac{4z^3}{3h^2}\left(\psi + \frac{1}{\alpha_1}\frac{\partial w}{\partial \xi_1}\right), \tag{2a}$$

$$u_2 = \frac{1}{\alpha_2}(L_2 v) + z\phi - \frac{4z^3}{3h^2}\left(\phi + \frac{1}{\alpha_2}\frac{\partial w}{\partial \xi_2}\right), \tag{2b}$$

$$u_3 = w, \tag{2c}$$

where (u_1, u_2, u_3) are the displacements along ξ_1, ξ_2 and z directions, respectively, (u, v, w) are the displacements of a point on the midplane, and ψ and ϕ are the rotations of normals to the midsurface with respect to the ξ_2- and ξ_1-axes. All displacement components (u, v, w, ψ, ϕ) are functions of ξ_1, ξ_2 and time t.

Using the linear strain–displacement relations referred to an orthogonal curvilinear coordinate system, we obtain:

$$\varepsilon_i = \varepsilon_i^{(0)} + z(k_i^0 + \gamma z^2 k_i^2), \quad \varepsilon_3 = 0, \quad \varepsilon_j = \varepsilon_j^{(0)} + \gamma z^2 k_j^1 \quad (i = 1, 2, 6;\ j = 4, 5) \tag{3a}$$

where

$$\begin{aligned}
&\varepsilon_1^{(0)} = \frac{1}{\alpha_1}\frac{\partial u}{\partial \xi_1} + \frac{w}{R_1}, \quad \varepsilon_2^{(0)} = \frac{1}{\alpha_2}\frac{\partial v}{\partial \xi_2} + \frac{w}{R_2}, \quad \varepsilon_4^{(0)} = \frac{1}{\alpha_2}\frac{\partial w}{\partial \xi_2} + \phi,\\
&\varepsilon_5^{(0)} = \frac{1}{\alpha_1}\frac{\partial w}{\partial \xi_1} + \psi, \quad \varepsilon_6^{(0)} = \frac{1}{\alpha_1}\frac{\partial v}{\partial \xi_1} + \frac{1}{\alpha_2}\frac{\partial u}{\partial \xi_2}, \quad k_1^0 = \frac{1}{\alpha_1}\frac{\partial \psi}{\partial \xi_1},
\end{aligned} \tag{3b}$$

$$\begin{aligned}
&k_2^0 = \frac{1}{\alpha_2}\frac{\partial \phi}{\partial \xi_2}, \quad k_6^0 = \frac{1}{\alpha_1}\frac{\partial \phi}{\partial \xi_1} + \frac{1}{\alpha_2}\frac{\partial \psi}{\partial \xi_2}, \quad k_1^2 = \frac{-n_2}{\alpha_1}\frac{\partial \varepsilon_5^{(0)}}{\partial \xi_1},\\
&k_2^2 = \frac{-n_2}{\alpha_2}\frac{\partial \varepsilon_4^{(0)}}{\partial \xi_2}, \quad k_4^1 = -n_1\left(\frac{1}{\alpha_2}\frac{\partial w}{\partial \xi_2} + \phi\right), \quad k_5^1 = -n_1\left(\frac{1}{\alpha_1}\frac{\partial w}{\partial \xi_1} + \psi\right),\\
&k_6^2 = -n_2\left(\frac{2}{\alpha_1 a_2}\frac{\partial^2 w}{\partial \xi_1 \partial \xi_2} + \frac{1}{\alpha_1}\frac{\partial \phi}{\partial \xi_1} + \frac{1}{\alpha_2}\frac{\partial \psi}{\partial \xi_2}\right), \quad n_1 = 3n_2 = 4/h^2.
\end{aligned} \tag{3c}$$

The governing equations associated with the displacement field (2a)–(2c) may be obtained using the dynamic version of the virtual displacement principle in the form [20].

$$\frac{1}{\alpha_1}\frac{\partial N_1}{\partial \xi_1}+\frac{1}{\alpha_2}\frac{\partial N_6}{\partial \xi_2}=\overline{I}_1\ddot{u}+\overline{I}_2\ddot{\psi}-\frac{\gamma\overline{I}_3}{\alpha_1}\frac{\partial \ddot{w}}{\partial \xi_1}, \tag{4a}$$

$$\frac{1}{\alpha_1}\frac{\partial N_6}{\partial \xi_1}+\frac{1}{\alpha_2}\frac{\partial N_2}{\partial \xi_2}=\overline{I}'_1\ddot{v}+\overline{I}'_2\ddot{\phi}-\frac{\gamma\overline{I}'_3}{\alpha_2}\frac{\partial \ddot{w}}{\partial \xi_2}, \tag{4b}$$

$$\begin{aligned}&\frac{1}{\alpha_1}\frac{\partial Q_1}{\partial \xi_1}+\frac{1}{\alpha_2}\frac{\partial Q_2}{\partial \xi_2}+q-\gamma n_1\left(\frac{1}{\alpha_1}\frac{\partial K_1}{\partial \xi_1}+\frac{1}{\alpha_2}\frac{\partial K_2}{\partial \xi_2}\right)+\gamma n_2\left(\frac{1}{\alpha_1^2}\frac{\partial^2 p_1}{\partial \xi_1^2}+\frac{2}{\alpha_1\alpha_2}\frac{\partial^2 p_6}{\partial \xi_1\partial \xi_2}+\frac{1}{\alpha_2^2}\frac{\partial^2 p_2}{\partial \xi_2^2}\right)-\frac{N_1}{R_1}-\frac{N_2}{R_2}\\&\quad=I_1\ddot{w}+\gamma\left(\overline{I}_3\frac{1}{\alpha_1}\frac{\partial \ddot{u}}{\partial \xi_1}+\frac{\overline{I}_5}{\alpha_1}\frac{\partial \ddot{\psi}}{\partial \xi_1}+\frac{\overline{I}'_3}{\alpha_2}\frac{\partial \ddot{v}}{\partial \xi_2}+\frac{\overline{I}'_5}{\alpha_2}\frac{\partial \ddot{\phi}}{\partial \xi_2}-n_2^2 I_7\left(\frac{1}{\alpha_1^2}\frac{\partial^2 \ddot{w}}{\partial \xi_1^2}+\frac{1}{\alpha_2}\frac{\partial \ddot{w}}{\partial \xi_2}\right)\right),\end{aligned} \tag{4c}$$

$$\frac{1}{\alpha_1}\frac{\partial M_1}{\partial \xi_1}+\frac{1}{\alpha_2}\frac{\partial M_6}{\partial \xi_2}-Q_1+\gamma n_1K_1-\gamma n_2\left(\frac{1}{\alpha_1}\frac{\partial p_1}{\partial \xi_1}+\frac{1}{\alpha_2}\frac{\partial p_2}{\partial \xi_2}\right)=\overline{I}_2\ddot{u}+\overline{I}_4\ddot{\psi}-\frac{\gamma\overline{I}_5}{\alpha_1}\frac{\partial \ddot{w}}{\partial \xi_1}, \tag{4d}$$

$$\frac{1}{\alpha_1}\frac{\partial M_6}{\partial \xi_1}+\frac{1}{\alpha_2}\frac{\partial M_2}{\partial \xi_2}-Q_2+\gamma n_1K_2-\gamma n_2\left(\frac{1}{\alpha_1}\frac{\partial p_6}{\partial \xi_1}+\frac{1}{\alpha_2}\frac{\partial p_2}{\partial \xi_2}\right)=\overline{I}'_2\ddot{v}+\overline{I}'_4\ddot{\phi}-\frac{\gamma\overline{I}'_5}{\alpha_2}\frac{\partial \ddot{w}}{\partial \xi_2}, \tag{4e}$$

where

$$\overline{I}_1=I_1+\gamma\frac{2}{R_1}I_2,\quad \overline{I}_2=I_2+\gamma\frac{1}{R_1}I_3-\gamma n_2I_4-\gamma\frac{n_2}{R_1}I_5,\quad \overline{I}_3=n_2I_4+\gamma\frac{n_2}{R_1}I_5,$$

$$\overline{I}_4=I_3-2\gamma n_2I_5+\gamma n_2^2I_7,\quad \overline{I}_5=n_2I_5-\gamma n_2^2I_7,\quad I_n=\sum_{k=1}^{N}\int_{z_{k-1}}^{z_k}\rho^{(k)}z^{n-1}\,\mathrm{d}z.$$

the quantities $\overline{I}'_i$ have the same forms as $\overline{I}_i$ except that R_1 is replaced by R_2, q is a force distributed over the upper surface of the shell, $\rho^{(k)}$ is the material density of the kth layer. The stress resultants are related to the strain components by the following laminate constitutive equations,

$$\begin{bmatrix}N_i\\M_i\\P_i\end{bmatrix}=\begin{bmatrix}A_{ij}&B_{ij}&\gamma E_{ij}\\B_{ij}&D_{ij}&\gamma F_{ij}\\E_{ij}&F_{ij}&H_{ij}\end{bmatrix}\begin{bmatrix}\varepsilon_j^{(0)}\\k_j^0\\k_j^2\end{bmatrix}\quad (i,j=1,2,6), \tag{5a}$$

$$\begin{bmatrix}Q_i\\K_i\end{bmatrix}=\begin{bmatrix}A_{ij}&\gamma D_{ij}\\D_{ij}&F_{ij}\end{bmatrix}\begin{bmatrix}\varepsilon_j^{(0)}\\k_j^1\end{bmatrix}\quad (i,j=4,5). \tag{5b}$$

The material elastic constants $C_{ij}^{(k)}$ of the kth lamina are related to the homogeneous laminate stiffnesses A_{ij}, B_{ij} etc., by the following expressions:

$$(A_{ij},B_{ij},D_{ij},E_{ij},F_{ij},H_{ij})=\sum_{k=1}^{N}\int_{z_{k-1}}^{z_k}C_{ij}^{(k)}(1,z,z^2,z^3,z^4,z^6)\,\mathrm{d}z\quad (i,j=1,2,4,5,6). \tag{6}$$

The present control problem accounts for various cases of boundary conditions at the edges, i.e., when the shell edges are simply supported (S), clamped (C) free (F), or when combination of these boundary conditions are prescribed over the edges. Then, these boundary conditions on the edges perpendicular to ξ_1-curve associated with the present shell theory take the form:

$$\begin{aligned}&S: v=w=\psi=N_1=M_1=P_1=0,\\&C: u=v=w=\psi=\phi=w_{,\xi_1}=0,\\&F: N_1=M_1=P_1=N_6=M_6-P_6=\widehat{Q}_1+P_{1,\xi_1}+P_{6,\xi_2}=0,\end{aligned} \tag{7}$$

where $(\ )_{,\xi_1}$ denotes partial differentiation with respect to ξ_1.

Governing Eqs. (4a)–(4e) can be specialized for flat plates by setting $1/R_1=1/R_2=0$, for spherical shells by setting $R_1=R_2=R$; and for cylindrical shells by setting $1/R_1=0$, $R_2=R$, and ξ_1-axis is taken along the generator of the cylinder. Governing equations of the first-order shear deformation (FST) can be deduced from those of the third-order theory (HST) by setting $\gamma=0$. Also the classical theory (CST) is obtained from FST by setting

$$\psi=-\frac{1}{\alpha_1}\frac{\partial w}{\partial \xi_1}\quad\text{and}\quad \phi=-\frac{1}{\alpha_2}\frac{\partial w}{\partial \xi_2}.$$

3. The control objective and optimization variables

The present study aims to minimize the dynamic response of a laminated doubly curved shell in a specified time $0 \leqslant t \leqslant \tau \leqslant \infty$ with the minimum possible expenditure of force $q(\xi_1, \xi_2, t)$. The total energy of the shell may be taken as a measure of the dynamic response so that the control objective may be written as

$$J(q, h_k, \theta_k) = \frac{1}{2}\int_0^{\infty}\int_0^{b}\int_0^{a}\int_{-\frac{h}{2}}^{\frac{h}{2}}\left[\varepsilon_i\sigma_i + \rho^{(k)}(\dot{u}_1^2 + \dot{u}_2^2 + \dot{u}_3^2)\right]\alpha_1\alpha_2\,\mathrm{d}z\,\mathrm{d}\xi_1\,\mathrm{d}\xi_2\,\mathrm{d}t + \mu\int_0^{\tau}\int_0^{b}\int_0^{a} q^2(\xi_1, \xi_2, t)\alpha_1\alpha_2\,\mathrm{d}\xi_1\,\mathrm{d}\xi_2\,\mathrm{d}t \quad (i = 1, 2, 4, 5, 6), \tag{8}$$

where a and b are curvilinear dimensions of the shell along ξ_1- and ξ_2-axes, respectively and the weighting factor μ is a positive constant. The last term in (8) is a penalty functional involving the control function $q \in L^2$ where L^2 denotes the set of all bounded square integrable functions on the domain of the solution.

The cost functional (8) of the present control problem depends on the distributed force $q(\xi_1, \xi_2, t)$, the thickness of the layers h_k and fiber orientation angle θ_k. Then the present optimal control problem can be reduced to determine the optimization variables q, h_k, and θ_k that minimize the cost functional (8).

4. Solution procedure

The solution of the system of partial differential Eqs. (4a)–(4e) with the boundary conditions (7), may be expanded in the form of double series in terms of the free vibration eigenfunctions of the shell. Then, the displacements functions (u, v, w, ψ, ϕ) and the closed-loop control function q may be represented as:

$$(u, v, w, \psi, \phi, q) = \sum_{m,n}\left(U_{mn}XY_{,\xi_2}, V_{mn}X_{,\xi_1}Y, W_{mn}XY, \Psi_{mn}X_{,\xi_1}Y, \Phi_{mn}XY_{,\xi_2}, Q_{mn}XY\right), \tag{9}$$

where U_{mn}, V_{mn}, W_{mn}, Ψ_{mn}, Φ_{mn} and Q_{mn} are unknown functions of time. The functions $X(\xi_1)$ and $Y(\xi_2)$ are continuous orthonormed functions which satisfy at least the geometric boundary conditions given in (7) and represent approximate shapes of the deflected surface of the vibrating shell. These functions, for different cases of boundary conditions are given in Appendix A.

Using Eqs. (3a), (3b), (3c), (5a) and (5b), we can get the governing Eqs. (4a)–(4e) in terms of the displacements. For these equations, the in-plane inertia terms may be neglected. Substituting expressions (9) into the resulting equations and multiplying each equation by the corresponding eigenfunction, then integrating over the domain of solution, we obtain after some mathematical manipulations, the following time equations:

$$\begin{bmatrix} U_1 & V_1 & W_1 & \Psi_1 & \Phi_1 \\ U_2 & V_2 & W_2 & \Psi_2 & \Phi_2 \\ U_3 & V_3 & W_3 & \Psi_3 & \Phi_3 \\ U_4 & V_4 & W_4 & \Psi_4 & \Phi_4 \\ U_5 & V_5 & W_5 & \Psi_5 & \Phi_5 \end{bmatrix}\begin{bmatrix} U_{mn} \\ V_{mn} \\ W_{mn} \\ \Psi_{mn} \\ \Phi_{mn} \end{bmatrix} = \begin{bmatrix} \overline{W}_1 \\ \overline{W}_2 \\ \overline{W}_3\ddot{W}_{mn} - Q_{mn} \\ \overline{W}_4\ddot{W}_{mn} \\ \overline{W}_5\ddot{W}_{mn} \end{bmatrix}, \tag{10}$$

the coefficients U_i, V_i, W_i, Φ_i, Ψ_i and $\overline{W}_i (i = 1, 2, \ldots, 5)$ are given in Appendix A. Solving the system (10), one gets an equation of the time-dependent functions W_{mn} and Q_{mn} only,

$$\ddot{W}_{mn} + \omega_{mn}^2 W_{mn} = l_{m,n}Q_{mn}, \quad \omega_{mn}^2 = \frac{\Delta_{mn}}{\Delta_{1mn}}, \quad l_{mn} = \frac{\Delta_0}{\Delta_{1mn}}, \tag{11}$$

where, Δ_{mn}, Δ_{1mn} and Δ_0 are given in the Appendix B.

Following previous analogous steps, we can get the objective functional (8) in the final form:

$$J = \sum_{m,n}\int_0^{\infty}\left(k_1W_{mn}^2 + k_2W_{mn}Q_{mn} + k_3Q_{mn}^2 + k_4\dot{W}_{mn}^2 + k_5\dot{W}_{mn}\dot{Q}_{mn} + k_6\dot{Q}_{mn}^2\right)\mathrm{d}t, \tag{12}$$

where, the coefficients k_i $(i = 1, 2, \ldots 6)$ are given in Appendix C. Since the system of Eq. (11) is separable, hence the functional (12) depends only on the variables found in (m, n)th equation of the system. With the aid of this condition, the problem is reduced to a problem of analytical design of controllers [21,22] for every $m, n = 1, 2, \ldots \infty$.

Now the optimal control problem is to find firstly, the control function $q_{mn}^{\mathrm{opt}}(t)$ that satisfies the conditions

$$J\left(q_{mn}^{\mathrm{opt}}\right) \leqslant J(q_{mn}) \quad \text{for all } q_{mn}(t) \in L^2([0, \infty]),$$

that is

$$\min_{q_{mn}} J = \min \sum J_{mn} = \sum_{m,n} \min_{q_{mn}\in L^2} J,$$

and, secondly, to find the optimum values of h_k and θ_k from the following minimization condition:

$$J\left(q_{mn}^{\text{opt}}, h_k^{\text{opt}}, \theta_k^{\text{opt}}\right) = \min_{h_k,\theta_k} I\left(q_{mn}^{\text{opt}}, h_k, \theta_k\right), \quad \sum_k h_k = h, \quad 0 < \theta < \pi/2.$$

For this problem, Liapunov–Bellman theory [22] is used to determine the control force $q(x, y, t)$. This theory gives the necessary and sufficient conditions for minimizing the functional (12) in the form:

$$\min_q \left[\frac{\partial L_{mn}}{\partial W_{mn}} \dot{W}_{mn} + \frac{\partial L_{mn}}{\partial \dot{W}_{mn}} \ddot{W}_{mn} + \overline{J}_{mn}\right] = 0, \tag{13}$$

provided that the Liapunov function

$$L_{mn} = A_{mn} W_{mn}^2 + 2B_{mn} W_{mn} \dot{W}_{mn} + C_{mn} \dot{W}_{mn}^2, \tag{14}$$

is positive definite, i.e., $A_{mn} > 0$, $C_{mn} > 0$ and $A_{mn} C_{mn} > B_{mn}^2$, where $\overline{J}_{mn}$ is the integrand of (12). Using Eq. (14) we can obtain the optimal control function in the form:

$$Q_{mn}^{\text{opt}} = \frac{-1}{2k_3}(2B_{mn} l_{mn} + k_2) W_{mn} - \frac{C_{mn} l_{mn}}{k_3} \dot{W}_{mn}, \tag{15}$$

then, substituting Eq. (15) into (13) and equating the coefficients of W_{mn}^2, $\dot{W}_{mn}^2$ and $W_{mn}\dot{W}_{mn}$ by zeros, the following system of equations is obtained

$$\begin{aligned}
&C_{mn}^2(a_1 B_{mn}^2 + a_2 B_{mn} + a_3) + a_4 B_{mn} + a_5 = 0,\\
&C_{mn}^2(a_6 C_{mn}^2 + a_7 B_{mn} + a_8) + a_9 B_{mn}^2 + a_{10} B_{mn} + a_{11} = 0,\\
&a_{12} A_{mn} + C_{mn}(a_{13} C_{mn}^2 + a_{14} C_{mn}^2 B_{mn} + a_{15} B_{mn}^2 + a_{16} B_{mn} + a_{17}) = 0,
\end{aligned} \tag{16}$$

where a_i $(i = 1, 2, \ldots, 17)$ are given in Appendix C. Under the condition that the Liapunov function is a positive definite, the solution of the system of nonlinear algebraic Eq. (16) may be obtained, then, using this solution into Eq. (11), one gets:

$$\ddot{W}_{mn} + \alpha_{mn} \dot{W}_{mn} + \beta_{mn}^2 W_{mn} = 0, \quad \alpha_{mn} = \frac{C_{mn} l_{mn}^2}{k_3}, \quad \beta_{mn}^2 = \omega_{mn}^2 + \frac{l_{mn}}{2k_3}(2B_{mn} l_{mn} + k_2),$$

the solution of this equation when $2\beta_{mn} > \alpha_{mn}$ is given by

$$W_{mn} = \mathrm{e}^{\frac{-\alpha_{mn} t}{2}}[\delta_{mn} \cos(\omega_{mn}^* t) + \tau_{mn} \sin(\omega_{mn}^* t)], \quad v_{mn} = \sqrt{\beta_{mn}^2 - \frac{1}{4}\alpha_{mn}^2},$$

where δ_{mn}, τ_{mn} are unknown coefficients which may be obtained from the initial conditions by expanding it in a series. If the initial conditions have the form:

$$w(\xi_1, \xi_2, 0) = \overline{A}(\xi_1, \xi_2), \quad \dot{w}(\xi_1, \xi_2, 0) = 0,$$

then, the controlled deflection solution takes the form:

$$W_{mn} = \overline{A}\mathrm{e}^{\frac{-\alpha_{mn} t}{2}}\left(\cos(\omega_{mn}^* t) + \frac{\alpha_{mn}}{2\omega_{mn}^*} \sin(\omega_{mn}^* t)\right). \tag{17}$$

Insert expressions (17) into (10), (12) and (15) we can get the controlled displacements, the total energy and the optimal control force. Then, we complete the minimization process for the dynamic response of the shell by determining the optimal design of the shell using the design variables θ_k and h_k.

5. Numerical results and discussion

Numerical results for maximum optimal control force q, central controlled deflection w and total energy J are presented for symmetric (or antisymmetric) angle-ply spherical and cylindrical shells with various cases of the boundary conditions (7). All layers of the laminate are assumed to be of the same orthotropic materials. A shear correction factor for FST is taken to be 5/6. The plane reduced stress material stiffnesses C_{ij} are given by

$$C_{11} = \frac{E_1}{1 - v_{12}v_{21}}, \quad C_{12} = \frac{v_{12}E_2}{1 - v_{12}v_{21}}, \quad C_{22} = \frac{E_2}{1 - v_{12}v_{21}},$$
$$C_{44} = G_{23}, \quad C_{55} = G_{13}, \quad C_{66} = G_{12}, \qquad v_{ij}E_j = v_{ji}E_i \quad (i,j = 1,2).$$

where E_i are Young's moduli; v_{ij} are Poisson's ratios and G_{ij} are shear moduli. In all calculations, unless otherwise stated, the following parameters are used:

$$a = b = 20 \text{ in.}, \quad h = 2 \text{ in.}, \quad \rho = 0.00012 \text{ lb} - s^2/\text{in.}^4, \quad R_1 = R_2 = 5a, \quad \mu = 0.001,$$
$$\overline{A} = 10^3 l\omega^{-2}, \quad E_2 = 10^6 \text{ psi}, \quad E_1 = 25E_2, \quad G_{12} = G_{13} = 0.5E_2, \quad G_{23} = 0.2E_2, \quad v_{12} = 0.25.$$

For the optimal design, we consider angle-ply $(\theta, 0, \theta)$ laminated shells with outer layers having the same thickness; and therefore we take the optimization thickness variable r representing the ratio of the outer layer thickness to the total shell thickness. All calculations in tables and figures are carried out at the midpoint of the shell, and for maximum amplitude of w and q.

Table 1 contains numerical results of controlled central deflection w, controlled energy J and maximum control force q obtained using the various shell theories CST, FST and HST for three-, five- and thirteen-layer symmetric spherical and cylindrical shells with simply-supported edges (SSSS). Table 2 contains similar results for two-, four- and twelve-layer antisymmetric spherical and cylindrical shells. The CST under-predicts w, J and q due to the assumed infinite rigidity of the transverse normals, hence, the CST models the structure stiffer than it is, so, the structure needs less energy to control its dynamic response. But, the results predicted by various shell theories are very close for thin shells, while, the discrepancy between them are pronounced for thicker shells. Note that the deflections obtained by CST differ from those obtained using FST and HST for the symmetric case by 40% for $h/a = 0.1$, and by 75% for $h/a = 0.2$. Further, in the antisymmetric case, these differences are less, where their maximum reaches 50% for $a/h = 0.2$. The differences between FST and HST results do not exceed 10% for moderately thick shells. Also, these

Table 1
Values of q, J and w for three-, five- and thirteen-layer symmetric SSSS spherical and cylindrical shells according to CST, FST and HST, $a = b = 20$, $R = 100$, $E_1/E_2 = 25$

h	Th.	45,0,45			45, −45, 0, −45, 45			45, −45, 45, −45, 45, −45/0/sym.		
		q	J	w	q	J	w	q	J	w
Case 1: spherical shell										
0.5	CST	487.20	45.312	1.2577	474.75	40.580	1.1395	465.07	37.269	1.0556
	FST	489.11	46.090	1.2769	476.51	41.216	1.1556	466.70	37.807	1.0694
	HST	489.53	46.271	1.2813	476.86	41.353	1.1590	467.00	37.915	1.0721
1	CST	307.19	12.945	0.2824	301.44	12.260	0.2680	297.25	11.781	0.2579
	FST	318.49	14.393	0.3129	312.21	13.576	0.2958	307.53	12.993	0.2836
	HST	320.85	14.720	0.3197	314.27	13.848	0.3015	309.35	13.226	0.2884
2	CST	145.91	2.7797	0.0441	144.27	2.7087	0.0430	143.32	2.6683	0.0423
	FST	175.09	4.2664	0.0676	172.80	4.1355	0.0656	171.21	4.0466	0.0642
	HST	180.34	4.5861	0.0726	177.49	4.4151	0.0699	175.46	4.2965	0.0681
4	CST	58.380	0.52759	0.0059	57.917	0.5189	0.0058	57.731	0.51545	0.0057
	FST	100.23	1.7015	0.0192	99.276	1.6665	0.0188	98.602	1.6422	0.0185
	HST	105.76	1.9195	0.0216	104.17	1.8572	0.0209	103.05	1.8141	0.0204
Case 2: cylindrical shell										
0.5	CST	560.49	88.807	2.2595	553.97	83.491	2.1439	549.20	79.818	2.0630
	FST	563.89	91.727	2.3223	557.26	86.126	2.2014	552.37	82.234	2.1162
	HST	564.65	92.415	2.3370	557.94	86.697	2.2137	552.98	82.722	2.1269
1	CST	331.94	16.296	0.3527	329.02	15.866	0.3437	327.36	15.624	0.3387
	FST	346.84	18.658	0.4015	343.72	18.140	0.3909	341.82	17.829	0.3844
	HST	350.01	19.209	0.4128	346.60	18.628	0.4008	344.45	18.269	0.3934
2	CST	149.99	2.9636	0.0470	148.91	2.9146	0.0462	148.50	2.8959	0.0459
	FST	182.58	4.7180	0.0747	181.28	4.6381	0.0735	180.60	4.5962	0.0728
	HST	188.62	5.1122	0.0809	186.79	4.9927	0.0790	185.68	4.9211	0.0779
4	CST	58.819	0.53623	0.0060	58.427	0.52873	0.0059	58.314	0.52655	0.0059
	FST	102.77	1.7982	0.0203	102.18	1.7759	0.0200	101.85	1.7631	0.0199
	HST	108.78	2.0435	0.0230	107.57	1.9940	0.0225	106.80	1.9627	0.0221

Table 2
Values of q, J and w for two-, four- and twelve-layer antisymmetric SSSS spherical and cylindrical shells according to CST, FST and HST, $a = b = 20$, $R = 100$, $E_1/E_2 = 25$

h	Th.	$45, -45$			$45, -45, 45, -45$			$45, -45, 45, -45, 45, -45$/antisym.		
		q	J	w	q	J	w	q	J	w
Case 1: spherical shell										
0.5	CST	411.23	23.302	0.6867	398.99	20.944	0.6218	395.60	20.334	0.6049
	FST	411.39	23.333	0.6879	399.66	21.067	0.6252	396.47	20.490	0.6092
	HST	411.38	23.336	0.6876	399.80	21.098	0.6260	396.63	20.522	0.6101
1	CST	302.91	12.435	0.2717	272.63	9.2634	0.2042	265.39	8.6119	0.1902
	FST	304.58	12.636	0.2760	278.13	9.7881	0.2156	272.13	9.2208	0.2034
	HST	304.60	12.647	0.2762	279.32	9.9099	0.2181	273.31	9.3366	0.2059
2	CST	182.60	4.6965	0.0741	144.37	2.7136	0.0430	137.06	2.4112	0.0383
	FST	191.92	5.3088	0.0838	164.47	3.6816	0.0584	159.74	3.4400	0.0547
	HST	192.11	5.3337	0.0842	168.21	3.8887	0.0617	163.12	3.6191	0.0575
4	CST	85.982	1.1910	0.0131	61.330	0.5843	0.0065	57.270	0.5070	0.0056
	FST	108.44	2.0134	0.0226	95.959	1.5477	0.0175	94.257	1.4895	0.0168
	HST	108.53	2.0290	0.0228	100.80	1.7290	0.0195	98.182	1.6329	0.0184
Case 2: cylindrical shell										
0.5	CST	549.04	79.737	2.0617	514.88	58.186	1.5698	506.27	53.829	1.4662
	FST	549.52	80.097	2.0697	516.62	59.116	1.5918	508.46	54.905	1.4920
	HST	549.53	80.117	2.0701	517.02	59.346	1.5971	508.88	55.125	1.4971
1	CST	389.90	27.306	0.5754	327.26	15.614	0.3386	314.30	13.852	0.3018
	FST	393.93	28.294	0.5951	337.59	17.166	0.3708	326.39	15.498	0.3363
	HST	394.05	28.343	0.5959	339.91	17.541	0.3785	328.60	15.826	0.3431
2	CST	210.15	6.6196	0.1040	156.36	3.2623	0.0517	147.12	2.8352	0.0450
	FST	225.39	7.9132	0.1243	183.48	4.7739	0.0756	176.90	4.3760	0.0694
	HST	225.79	7.9670	0.1250	188.86	5.1275	0.0811	181.64	4.6694	0.0740
4	CST	90.382	1.3267	0.0146	62.856	0.61535	0.0068	58.508	0.53030	0.0059
	FST	118.35	2.4438	0.0274	102.60	1.7915	0.0202	100.53	1.7140	0.0194
	HST	118.52	2.4665	0.0276	108.65	2.0385	0.0230	105.38	1.9065	0.0215

differences in the control force do not exceed 45% for the symmetric case and 25% for the antisymmetric case. In general, the symmetric laminated shells are more sensitive to the transverse shear effect than the antisymmetric ones. This is because that the angle-ply symmetric shells offer more shear stiffnesses than the antisymmetric shells, so, they exhibit bending-twisting coupling which has the effect of increasing the flexibility of the transverse normals.

The dependence of the control process on the number of layers N is illustrated in Tables 3 and 4, where the values of q, J and w are presented against the number of layers N for symmetric and antisymmetric shells with various cases of boundary conditions. These results show that the HST is believed to be more accurate than CST and FST for various cases of boundary conditions. Also, the number of layers has a weak effect on the damping process of the dynamic response for the symmetric shells, while, this effect is more obvious in antisymmetric shells. In general, the influence of the number of layers dies out rapidly when $N \geqslant 5$. The above observation can be explained by the fact that the symmetric shells exhibit no coupling between bending and extension, and this coupling appears in antisymmetric shells and makes them more flexible. Moreover, this coupling disappears as the number of layers increases. Note that, the cylindrical shells need more expenditure of control energy to reduce their dynamic responses than the symmetric ones of same material and geometry.

The variation of q, J and w against the radius of curvature R is presented in Table 5 for symmetric spherical and cylindrical shells with simply-supported edges. The previous conclusions about the discrepancy between the CST, FST and HST result still hold for the results in Table 5. In addition, this discrepancy increases as the radius of the shell increases. As it is known for shallow shells that the effect of shear deformation is weak, but the present results for shallow shells have high sensitivity to the shear deformation effect. This may be explained as for moderately thick shallow shell, the thickness has dominant effect more than the shell radius.

Tables 6–8 include optimum values of fiber orientation angle θ_{opt} and thickness ratio r_{opt} against side-to-thickness ratio, aspect ratio, and orthotropy ratio for $(\theta, 0, \theta)$ symmetric spherical and cylindrical shells in various cases of boundary conditions. Note that, for each case of boundary conditions, there is a suitable optimal design for the shell to

Table 3
Effect of number of layers N on q, J and w for symmetric $(45, -45 \ldots, 0 \ldots, -45, 45)$ shells according to CST, FST and HST with various boundary conditions, $a/b = 1$, $a/h = 5$, $E_1/E_2 = 25$, $R/h = 25$

N	Th.	CCSS			CCCC			CFSS		
		q	J	w	q	J	w	q	J	w
Case 1: spherical shell										
3	CST	88.451	0.4917	0.0053	149.78	0.5780	0.0061	278.86	18.928	0.0495
	FST	175.36	2.1637	0.0237	325.17	3.1381	0.0334	305.50	26.788	0.0745
	HST	182.03	2.3567	0.0258	339.34	3.4616	0.0368	314.06	29.378	0.0814
5	CST	89.031	0.4985	0.0054	149.89	0.5788	0.0061	288.96	20.726	0.0530
	FST	176.37	2.1913	0.0240	325.01	3.1348	0.0333	311.91	28.571	0.0790
	HST	182.96	2.3832	0.0261	338.12	3.4345	0.0365	318.45	30.806	0.0854
13	CST	89.210	0.5005	0.0054	149.91	0.5791	0.0061	297.84	22.456	0.0563
	FST	177.51	2.2222	0.0243	324.92	3.1321	0.0333	318.41	30.429	0.0835
	HST	184.48	2.4266	0.0266	337.52	3.4203	0.0363	321.38	31.827	0.0883
Case 1: cylindrical shell										
3	CST	89.192	0.5005	0.0054	150.76	0.5861	0.0061	305.67	24.312	0.0605
	FST	181.95	2.3484	0.0257	336.65	3.3928	0.0361	347.50	39.575	0.1025
	HST	189.52	2.5780	0.0282	352.54	3.7745	0.0401	361.20	45.445	0.1161
5	CST	89.727	0.5068	0.0055	150.81	0.5866	0.0061	306.40	24.357	0.0602
	FST	182.59	2.3667	0.0259	336.01	3.3784	0.0359	337.71	36.337	0.0963
	HST	190.01	2.5927	0.0284	350.64	3.7287	0.0396	346.54	40.023	0.1059
13	CST	89.851	0.5082	0.0055	150.81	0.5865	0.0061	306.49	24.350	0.0601
	FST	183.32	2.3874	0.0262	335.44	3.3654	0.0358	330.63	34.188	0.0922
	HST	191.09	2.6256	0.0287	349.46	3.7004	0.0393	334.19	35.983	0.0982

Table 4
Effect of number of layers N on q, J and w for antisymmetric $(45, -45, \ldots)$ shells according to CST, FST and HST with various boundary conditions, $a/b = 1$, $a/h = 5$, $E_1/E_2 = 25$, $R/h = 25$

N	Th.	CCSS			CCCC			CFSS		
		q	J	w	q	J	w	q	J	w
Case 1: spherical shell										
2	CST	134.70	1.1867	0.0127	227.75	1.3921	0.0144	243.48	15.603	0.0514
	FST	192.29	2.6443	0.0288	348.01	3.6462	0.0386	248.02	17.009	0.0581
	HST	192.14	2.6550	0.0290	347.40	3.6501	0.0387	246.09	16.793	0.0577
4	CST	95.644	0.5780	0.0062	161.43	0.67460	0.0071	233.39	12.782	0.0385
	FST	175.17	2.1583	0.0236	322.55	3.0812	0.0328	233.04	14.004	0.0467
	HST	184.45	2.4262	0.0265	339.70	3.4705	0.0368	231.19	13.998	0.0476
12	CST	89.241	0.5010	0.0054	150.59	0.58433	0.0061	229.97	12.092	0.0358
	FST	172.88	2.0970	0.0230	319.25	3.0111	0.0320	228.83	13.324	0.0444
	HST	179.94	2.2976	0.0252	331.91	3.2932	0.0350	227.53	13.372	0.0453
Case 2: cylindrical shell										
2	CST	138.68	1.2637	0.0135	232.40	1.4546	0.0151	320.28	31.833	0.0904
	FST	205.58	3.0717	0.0335	367.30	4.1227	0.0437	338.68	39.315	0.1135
	HST	205.53	3.0870	0.0336	366.68	4.1275	0.0437	334.79	38.286	0.1118
4	CST	97.035	0.5958	0.0064	163.05	0.68912	0.0072	287.94	21.295	0.0568
	FST	185.03	2.4365	0.0267	337.73	3.4166	0.0363	298.68	26.117	0.0767
	HST	196.14	2.7824	0.0304	357.70	3.9013	0.0414	297.01	26.306	0.0792
12	CST	90.374	0.5144	0.0056	151.89	0.59521	0.0062	279.81	19.336	0.0512
	FST	182.32	2.3588	0.0258	333.89	3.3306	0.0354	289.46	23.855	0.0708
	HST	190.76	2.6156	0.0286	348.53	3.6781	0.0391	288.75	24.174	0.0732

improve its performance. Further the dimensions of the shell with the orthotropy ratio have an important role at determining the optimal design. For example, the cross-ply lamination scheme with layers of equithickness is the

Table 5
Values of q, J and w for three-, five- and thirteen-layer symmetric SSSS spherical and cylindrical shells according to CST, FST and HST, $a/b = 1$, $a/h = 10$, $E_1/E_2 = 25$

R	Th.	45,0,45			$45, -45, 0, -45, 45$			$45, -45, 45, -45, 45, -45, /0/$sym.		
		q	J	w	q	J	w	q	J	w
Case 1: spherical shell										
10	CST	56.358	0.32451	0.004789	52.388	0.28023	0.004161	49.157	0.24836	0.003733
	FST	57.315	0.33671	0.004977	53.160	0.28941	0.004305	49.806	0.25566	0.003849
	HST	57.420	0.33844	0.005002	53.243	0.29065	0.004322	49.863	0.25654	0.003862
50	CST	132.60	2.2290	0.035302	129.51	2.1141	0.033500	127.24	2.0330	0.032233
	FST	152.74	3.0886	0.048948	148.35	2.8886	0.045807	144.98	2.7411	0.043507
	HST	156.06	3.2529	0.051518	151.18	3.0221	0.047900	147.41	2.8532	0.045267
100	CST	145.91	2.7796	0.044084	144.26	2.7086	0.042967	143.31	2.6680	0.042334
	FST	175.07	4.2655	0.067614	172.80	4.1350	0.065562	171.18	4.0453	0.064164
	HST	180.33	4.5860	0.072615	177.48	4.4147	0.069935	175.44	4.2951	0.068074
∞	CST	151.42	3.0300	0.048068	150.54	2.9898	.047434	150.32	2.9796	0.047273
	FST	185.28	4.8893	0.077459	184.37	4.8319	0.076564	184.04	4.8111	0.076243
	HST	191.66	5.3155	0.084110	190.21	5.2192	0.082604	189.48	5.1691	0.081827
Case 2: cylindrical shell										
10	CST	97.401	1.0213	0.0147	97.401	1.0213	0.0147	87.430	0.8219	0.0121
	FST	102.94	1.1543	0.0167	102.94	1.1543	0.0167	91.522	0.9088	0.0134
	HST	103.69	1.1744	0.0170	103.69	1.1744	0.0170	91.977	0.9199	0.0135
50	CST	146.36	2.7895	0.0441	146.36	2.7895	0.0441	143.68	2.6761	0.0423
	FST	175.62	4.2814	0.0676	175.62	4.2814	0.0676	171.64	4.0585	0.0642
	HST	180.89	4.6023	0.0726	180.89	4.6023	0.0726	175.91	4.3091	0.0681
100	CST	150.09	2.9659	0.0470	150.09	2.9659	0.0470	148.56	2.8972	0.0459
	FST	182.69	4.7216	0.0747	182.69	4.7216	0.0747	180.67	4.5984	0.0728
	HST	188.75	5.1162	0.0809	188.75	5.1162	0.0809	185.75	4.9235	0.0779
∞	CST	151.08	3.0137	0.0478	151.08	3.0137	0.0478	149.87	2.9586	0.0469
	FST	184.63	4.8467	0.0768	184.63	4.8467	0.0768	183.19	4.7571	0.0754
	HST	190.91	5.2637	0.0833	190.91	5.2637	0.0833	188.52	5.1060	0.0808

Table 6
Optimum values of θ_{opt} and r_{opt} for $(\theta, 0, \theta)$ spherical and cylindrical shell against a/h for various boundary conditions (BC), $E_1/E_2 = 25$, $R/a = 5$, $a/b = 1$

BC	Opt.	a/h									
		5	10	15	20	25	5	10	15	20	25
		Case 1: spherical shell					*Case 2: cylindrical shell*				
SSSS	θ_{opt}	45°	45°	45°	45°	45°	44.7	44.9°	45°	44.9°	44.9°
	r_{opt}	0.5	0.5	0.5	0.5	0.5	0.5	0.5	0.5	0.5	0.5
CSSS	θ_{opt}	33.1°	35.2°	35.6°	36.2°	36.7°	33°	36.9°	39.5°	41.6°	43.4°
	r_{opt}	0.31	0.41	0.5	0.5	0.5	0.27	0.41	0.49	0.5	0.5
CCSS	θ_{opt}	30°	27.1°	19.5°	9.6°	0°	31.1°	28.7°	21.9°	14.2°	8°
	r_{opt}	0.19	0.21	0.21	0.2	Open	0.21	0.23	0.23	0.25	0.38
CCCC	θ_{opt}	90°	90°	90°	90°	90°	63.7°	68.1°	90°	90°	90°
	r_{opt}	0.03	0.05	0.05	0.05	0.05	0.5	0.5	0.5	0.5	0.5
CFSS	θ_{opt}	90°	90°	90°	90°	90°	90°	90°	90°	90°	90°
	r_{opt}	0.5	0.28	0.12	0.06	0.01	0.5	0.5	0.5	0.5	0.5

optimal design for symmetric shells when $a/b \geqslant 3$, and when $a/h \geqslant 15$ in the CCCC and CFSS boundary conditions cases. Particularly, for large value of E_1/E_2.

Table 7
Optimum values of θ_{opt} and r_{opt} for $(\theta, 0, \theta)$ spherical and cylindrical shell against a/b for various boundary conditions (BC), $E_1/E_2 = 25$, $R/a = 5$, $a/h = 10$

BC	Opt.	a/b							
		1	2	3	4	1	2	3	4
		Case 1: spherical shell				*Case 2: cylindrical shell*			
SSSS	θ_{opt}	45°	79.9°	90°	90°	44.9°	80.2°	90°	90°
	r_{opt}	0.5	0.5	0.5	0.5	0.5	0.5	0.5	0.5
CSSS	θ_{opt}	35.2°	77.4°	90°	90°	36.9°	77.7°	90°	90°
	r_{opt}	0.41	0.5	0.5	0.5	0.41	0.5	0.5	0.5
CCSS	θ_{opt}	27.1°	77.2°	90°	90°	28.7°	77.5°	90°	90°
	r_{opt}	0.21	0.5	0.5	0.5	0.23	0.5	0.5	0.5
CCCC	θ_{opt}	90°	90°	90°	90°	68.1°	90°	90°	90°
	r_{opt}	0.05	0.07	0.5	0.5	0.5	0.5	0.5	0.5
CFSS	θ_{opt}	90°	90°	90°	90°	90°	90°	90°	90°
	r_{opt}	0.28	0.5	0.5	0.5	0.5	0.5	0.5	0.5

Table 8
Optimal quantities (opt.) for spherical and cylindrical shell against E_1/E_2 for various boundary conditions (BC), $a/h = 10$, $R/a = 5$, $a/b = 1$ (open = arbitrary)

BC	Opt.	E_1/E_2									
		1	5	10	25	40	1	5	10	25	40
		Case 1: spherical shell					*Case 2: cylindrical shell*				
SSSS	θ_{opt}	90°	45°	45°	45°	45°	90°	45°	44.9°	44.9°	44.8°
	r_{opt}	0.36	0.5	0.5	0.5	0.5	0.36	0.5	0.5	0.5	0.5
CSSS	θ_{opt}	90°	31.9°	33.5°	35.3°	36.3°	90°	32.8°	34.5°	36.9°	39.4°
	r_{opt}	0.28	0.43	0.42	0.41	0.42	0.28	0.43	0.41	0.41	0.43
CCSS	θ_{opt}	0°	0°	16.3°	27.0°	29.4°	0°	0°	17.7°	28.7°	31.8°
	r_{opt}	Open	Open	0.19	0.21	0.21	Open	Open	0.21	0.23	0.24
CCCC	θ_{opt}	45°	90°	90°	90°	90°	45°	90°	90°	68.1°	68.8°
	r_{opt}	0.5	0.03	0.04	0.05	0.04	0.5	0.5	0.5	0.5	0.5
CFSS	θ_{opt}	45.8°	90°	90°	90°	90°	46.1°	90°	90°	90°	90°
	r_{opt}	0.5	0.34	0.34	0.28	0.12	0.5	0.5	0.5	0.5	0.5

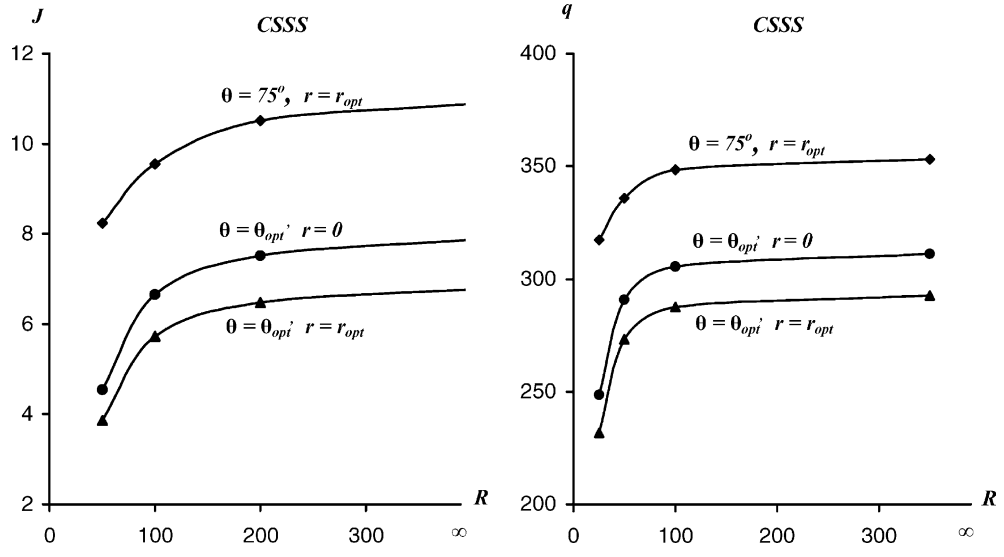

Fig. 1. Curves of J and q plotted against R for $(\theta, 0, \theta)$ CSSS spherical shell, $a/b = 1$, $a/h = 10$, $E_1/E_2 = 25$.

Figs. 1 and 2 display J- and q-curves against the radius R for $(\theta, 0, \theta)$ symmetric spherical and cylindrical shells with three different optimal designs, which are partially optimal design over the thickness ratio r, partially optimal design over the fiber orientation angle θ and optimal design over both θ and r. All the previous optimal designs considerably reduce the dynamic response of the shell as well as the maximum control force (or control energy). But, the optimal design over both θ and r is the most efficient. The effect of side-to-thickness ratio on the energy J and the control force q is presented in Fig. 3. The figure confirms the efficiency of the present optimal design over θ and r for all side-to-thickness ratios, particularly, for thinner shells ($a/h > 10$) which need more expenditure of energy to control its dynamic response. The dependence of J and q on the orthotropy ratio E_1/E_2 and aspect ratio a/b is presented in Figs. 4 and 5. These figures reveal that the shells may be tailored using E_1/E_2 and a/b to improve its performance, where J and q are rapidly decreasing with increasing the ratios E_1/E_2 and a/b. Thus the present optimization control may be extended to include four or five design variables.

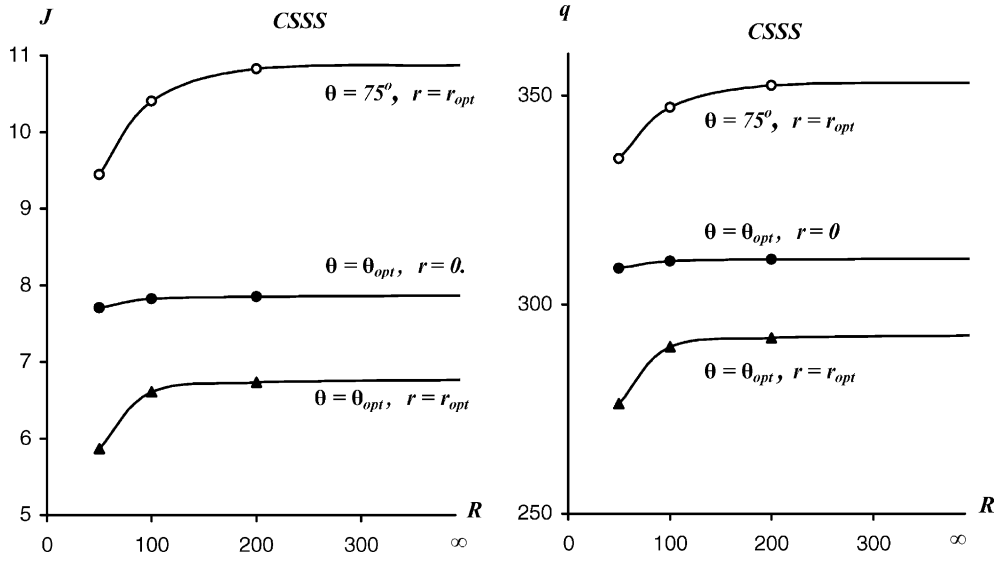

Fig. 2. Curves of J and q plotted against R for $(\theta, 0, \theta)$ CCSS cylindrical shell, $a/b = 1$, $a/h = 10$, $E_1/E_2 = 25$.

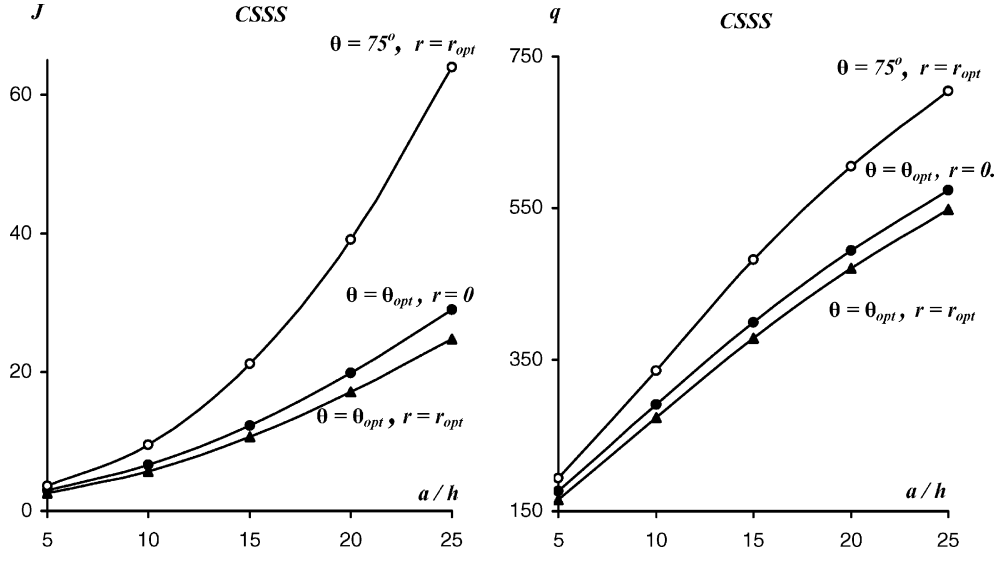

Fig. 3. Curves of J and q plotted against a/h for $(\theta, 0, \theta)$ CSSS spherical shell, $a/b = 1$, $E_1/E_2 = 25$, $R/h = 50$.

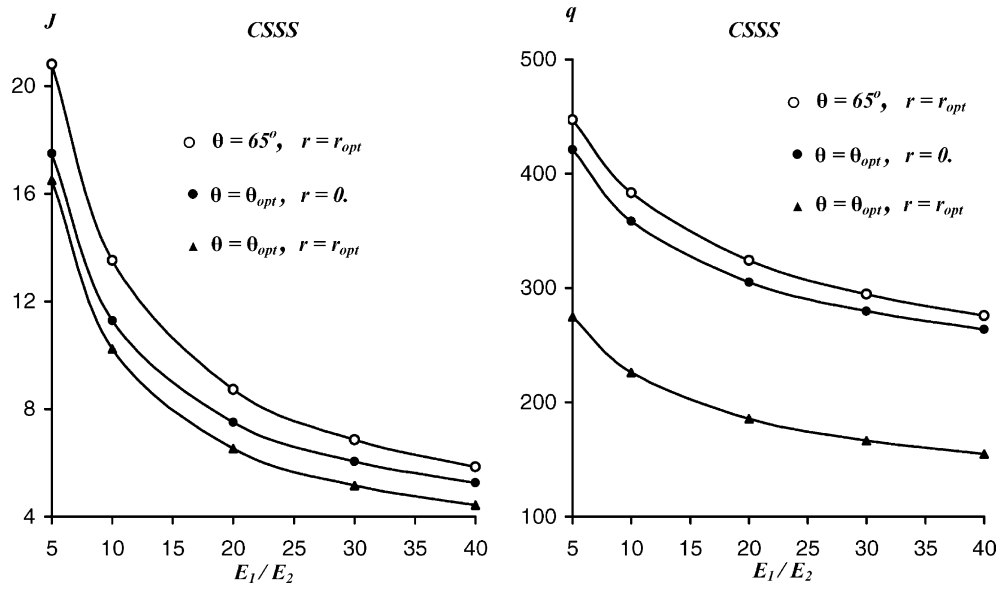

Fig. 4. Curves of J and q plotted against E_1/E_2 for $(\theta, 0, \theta)$ CSSS spherical shell, $a/b = 1$, $a/h = 10$, $R/h = 50$.

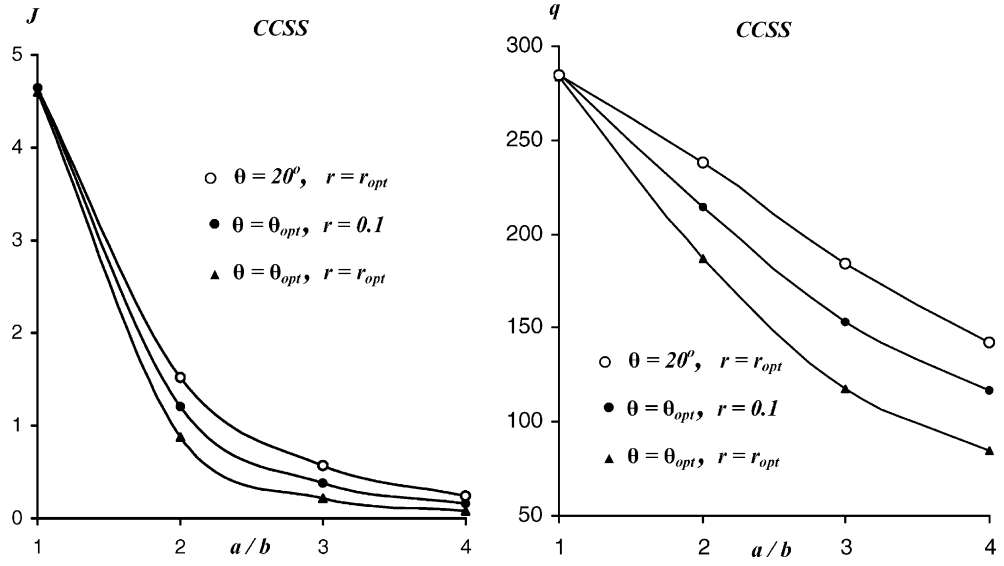

Fig. 5. Curves of J and q plotted against a/b for $(\theta, 0, \theta)$ CCSS spherical shell, $E_1/E_2 = 25$, $a/h = 10$, $R/h = 50$.

6. Conclusion

A structural and control optimization technique for minimizing the dynamic response of composite laminated doubly curved shells is presented. A higher-order shell theory is used to formulate the control objective for various cases of boundary conditions. Optimal levels of ply thickness, fiber orientation angle and closed-loop control force are determine for angle-ply orthotropic laminated spherical and cylindrical shells in various cases of boundary conditions. The discrepancy between the CST, FST and HST results is investigated by numerical examples. The effect of the transverse shear deformation on the control optimization process is studied for symmetric and antisymmetric shells. It is found that the optimization variables of the angle-ply symmetric laminated shells are more sensitive to the transverse shear effect than those of the antisymmetric ones. While, the number of layers has more effect on the antisymmetric shells than the symmetric ones. For each case of boundary conditions, there is a suitable optimal design for the shell to improve its performance. The present optimal control approach is believed to be more efficient.

Appendix A

$$
\begin{aligned}
&\text{SS}: X(\xi_1) = \sin\mu_m\alpha_1\xi_1, \quad \mu_m = m\pi/a.\\
&\text{CC}: X(\xi_1) = \sin\mu_m\alpha_1\xi_1 - \sinh\mu_m\alpha_1\xi_1 - \eta_m(\cos\mu_m\alpha_1\xi_1 - \cosh\mu_m\alpha_1\xi_1),\\
&\qquad \eta_m = (\sin\mu_m a - \sinh\mu_m a)/(\cos\mu_m a - \cosh\mu_m a), \quad \mu_m = (m+0.5)\pi/a.\\
&\text{CS}: X(\xi_1) = \sin\mu_m\alpha_1\xi_1 - \sinh\mu_m\alpha_1\xi_1 - \eta_m(\cos\mu_m\alpha_1\xi_1 - \cosh\mu_m\alpha_1\xi_1),\\
&\qquad \eta_m = (\sin\mu_m a + \sinh\mu_m a)/(\cos\mu_m a + \cosh\mu_m a), \quad \mu_m = (m+0.25)\pi/a.\\
&\text{CF}: X(\xi_1) = \sin\mu_m\alpha_1\xi_1 - \sinh\mu_m\alpha_1\xi_1 - \eta_m(\cos\mu_m\alpha_1\xi_1 - \cosh\mu_m\alpha_1\xi_1),\\
&\qquad \eta_m = (\sin\mu_m a + \sinh\mu_m a)/(\cos\mu_m a + \cosh\mu_m a), \quad \mu_1 = 1.875/a, \quad \mu_2 = 4.694/a,\\
&\qquad \mu_3 = 7.855/a, \quad \mu_4 = 10.996/a \quad \text{and} \quad \mu_m = (m-0.25)\pi/a, \quad \text{for } m \geqslant 5.
\end{aligned}
$$

Along ξ_2-axis these functions say $Y(\xi_2)$ are similar to $X(\xi_1)$ but ξ_1, a, m, μ_m and η_m can be replaced by ξ_2, b, n, μ_n and η_n respectively.

$$
\begin{aligned}
&U_1 = A_{11}e_9 + 2A_{16}e_{10} + A_{66}e_8, \quad \Psi_1 = \overline{s}_{66}e_{10} + 2\overline{s}_{16}e_9 + \overline{s}_{11}e_{11}, \quad V_1 = A_{26}e_{10} + (A_{66}+A_{12})e_9 + A_{16}e_{11},\\
&W_1 = s_{26}e_8 + (s_{12}+2s_{66})e_{10} + 3s_{16}e_9 + s_{11}e_{11} + \overline{R}_3e_{12} + \overline{R}_1e_5, \quad \Phi_1 = \overline{s}_{26}e_8 + (\overline{s}_{12}+\overline{s}_{66})e_{10} + \overline{s}_{16}e_9,\\
&U_2 = (A_{12}+A_{66})e_2 + A_{26}e_1 + A_{16}e_3, \quad V_2 = A_{22}e_2 + A_{66}e_4 + 2A_{26}e_3, \quad \Phi_2 = \overline{s}_{22}e_1 + \overline{s}_{66}e_3 + 2\overline{s}_{26}e_2,\\
&W_2 = s_{22}e_1 + 3s_{26}e_2 + (s_{12}+2s_{66})e_3 + s_{16}e_4 + \overline{R}_2e_5 + \overline{R}_3e_6, \quad \Psi_2 = (\overline{s}_{12}+\overline{s}_{66})e_3 + \overline{s}_{26}e_2 + \overline{s}_{16}e_4,\\
&U_3 = -s_{26}e_{17} - \overline{R}_3e_{16} - 3s_{16}e_{14} - \overline{R}_1e_5 - (s_{12}+2s_{66})e_1 - s_{11}e_{11},\\
&V_3 = -3s_{26}e_{14} - \overline{R}_3e_{13} - s_{16}e_{15} - (s_{12}+2s_{66})e_{11} - \overline{R}_2e_5 - s_{22}e_1,\\
&W_3 = -4\eta_{26}e_1 + 2(\zeta_{45}-2\overline{R}_6)e_5 - \overline{R}_7e_7 - 4\eta_{16}e_{11} + (\zeta_{55}-2\overline{R}_4)e_{13} - 2(\eta_{12}+2\eta_{66})e_{14} - \eta_{11}e_{15} + (\zeta_{44}-2\overline{R}_5)e_{16} - \eta_{22}e_{17},\\
&\Psi_3 = -\overline{\eta}_{26}e_1 + (\zeta_{45}-\overline{R}_6)e_5 - 3\overline{\eta}_{16}e_{11} + (\zeta_{55}-\overline{R}_4)e_{13} - (\overline{\eta}_{12}+2\overline{\eta}_{66})e_{14} - \overline{\eta}_{11}e_{15},\\
&\Phi_3 = -3\overline{\eta}_{26}e_1 + (\zeta_{45}-\overline{R}_6)e_5 - \overline{\eta}_{16}e_{11} + (\zeta_{44}-\overline{R}_5)e_{16} - (\overline{\eta}_{12}+2\overline{\eta}_{66})e_{14} - \overline{\eta}_{22}e_{17},\\
&U_4 = \overline{s}_{66}e_1 + 2\overline{s}_{16}e_2 + \overline{s}_{11}e_3, \quad V_4 = \overline{s}_{26}e_2 + (\overline{s}_{12}+\overline{s}_{66})e_3 + \overline{s}_{16}e_4,\\
&W_4 = \overline{\eta}_{26}e_1 + (\overline{\eta}_{12}+2\overline{\eta}_{66})e_2 + 3\overline{\eta}_{16}e_3 + \overline{\eta}_{11}e_4 + (\overline{R}_6-\zeta_{45})e_5 + (\overline{R}_4-\zeta_{55})e_6,\\
&\Psi_4 = \eta^*_{66}e_2 + 2\eta^*_{16}e_3 + \eta^*_{11}e_4 - \zeta_{55}e_6, \quad V_5 = \overline{s}_{22}e_{10} + \overline{s}_{66}e_{11} + 2\overline{s}_{26}e_9,\\
&\Phi_4 = \eta^*_{26}e_1 + (\eta^*_{12}+\eta^*_{66})e_2 + \eta^*_{16}e_3 - \zeta_{45}e_5, \quad U_5 = (\overline{s}_{12}+\overline{s}_{66})e_{10} + \overline{s}_{26}e_8 + \overline{s}_{16}e_9,\\
&W_5 = 3\overline{\eta}_{26}e_{10} + (\overline{\eta}_{12}+2\overline{\eta}_{66})e_9 + \overline{\eta}_{16}e_{11} + \overline{\eta}_{22}e_8 + (\overline{R}_6-\zeta_{45})e_5 + (\overline{R}_5-\zeta_{44})e_{12},\\
&\Psi_5 = \eta^*_{26}e_{10} + (\eta^*_{12}+\eta^*_{66})e_9 + \eta^*_{16}e_{11} - \zeta_{45}e_5, \quad \Phi_5 = \eta^*_{66}e_9 + 2\eta^*_{26}e_{10} + \eta^*_{22}e_8 - \zeta_{44}e_{12},\\
&\overline{W}_1 = \gamma\overline{I}_3e_5, \quad \overline{W}_2 = \gamma\overline{I}'_3e_5, \quad \overline{W}_3 = \gamma n_2^2 I_7(e_{13}+e_{16}) - I_1e_7, \quad \overline{W}_4 = \gamma\overline{I}_5e_6, \quad \overline{W}_5 = \gamma\overline{I}'_5e_{12},\\
&s_{ij} = -n_2\gamma E_{ij}, \quad \overline{s}_{ij} = s_{ij} + B_{ij}, \quad \eta_{ij} = n_2^2\gamma^2 H_{ij}, \quad \overline{\eta}_{ij} = \eta_{ij} - n_2\gamma F_{ij},\\
&\eta^*_{ij} = \eta_{ij} - 2n_2\gamma F_{ij} + D_{ij} \quad (i,j=1,2,6),\\
&\zeta_{ij} = n_1^2\gamma^2 F_{ij} - 2n_1\gamma D_{ij} + A_{ij} \quad (i,j=4,5),\\
&\overline{R}_1 = A_{11}/R_1 + A_{12}/R_2, \quad \overline{R}_2 = A_{12}/R_1 + A_{22}/R_2, \quad \overline{R}_3 = A_{16}/R_1 + A_{26}/R_2, \quad \overline{R}_4 = s_{11}/R_1 + s_{12}/R_2,\\
&\overline{R}_5 = s_{12}/R_1 + s_{22}/R_2, \quad \overline{R}_6 = s_{16}/R_1 + s_{26}/R_2, \quad \overline{R}_7 = A_{11}/R_1^2 + 2A_{12}/R_1R_2 + A_{22}/R_2^2,\\
&\overline{R}_8 = \overline{s}_{11}/R_1 + \overline{s}_{12}/R_2, \quad \overline{R}_9 = \overline{s}_{12}/R_1 + \overline{s}_{22}/R_2, \quad \overline{R}_{10} = \overline{s}_{16}/R_1 + \overline{s}_{26}/R_2.
\end{aligned}
$$

If $x = \alpha_1\xi_1$ and $y = \alpha_2\xi_2$, we have:

$$
\begin{aligned}
&(e_1,e_2,e_3,e_4,e_5,e_6) = \int_0^a\int_0^b (XY_{,yyy}, X_{,x}Y_{,yy}, X_{,xx}Y_{,y}, X_{,xxx}Y, XY_{,y}, X_{,x}Y)X_{,x}Y\,\mathrm{d}x\,\mathrm{d}y,\\
&(e_8,e_9,e_{10},e_{11},e_{12}) = \int_0^a\int_0^b (XY_{,yyy}, X_{,xx}Y_{,y}, X_{,x}Y_{,yy}, X_{,xxx}Y, XY_{,y})XY_{,y}\,\mathrm{d}x\,\mathrm{d}y,\\
&(e_7,e_{13},e_{14},e_{15},e_{16},e_{17}) = \int_0^a\int_0^b (XY, X_{,xx}Y, X_{,xx}Y_{,yy}, X_{,xxxx}Y, XY_{,yy}, XY_{,yyyy})XY\,\mathrm{d}x\,\mathrm{d}y,\\
&(e_{18},e_{19},e_{20}) = \int_0^a\int_0^b \left(X_{,x}^2Y_{,y}^2, X^2Y_{,yy}^2, X_{,xx}^2Y^2\right)\mathrm{d}x\,\mathrm{d}y.
\end{aligned}
$$

Appendix B

$$\Delta_{mn} = \Delta_{11}U_3 + \Delta_{21}V_3 + \Delta_{41}\Psi_3 + \Delta_{51}\Phi_3 - \Delta_0 W_3,$$
$$\Delta_{1mn} = \Delta_0\overline{W}_3 - \Delta_{12}U_3 - \Delta_{22}V_3 - \Delta_{42}\Psi_3 - \Delta_{52}\Phi_3,$$
$$\Delta_0 = \begin{vmatrix} U_1 & V_1 & \Psi_1 & \Phi_1 \\ U_2 & V_2 & \Psi_2 & \Phi_2 \\ U_4 & V_4 & \Psi_4 & \Phi_4 \\ U_5 & V_5 & \Psi_5 & \Phi_5 \end{vmatrix}, \quad \Delta_{11} = \begin{vmatrix} W_1 & V_1 & \Psi_1 & \Phi_1 \\ W_2 & V_2 & \Psi_2 & \Phi_2 \\ W_4 & V_4 & \Psi_4 & \Phi_4 \\ W_5 & V_5 & \Psi_5 & \Phi_5 \end{vmatrix}, \quad \Delta_{12} = \begin{vmatrix} \overline{W}_1 & V_1 & \Psi_1 & \Phi_1 \\ \overline{W}_2 & V_2 & \Psi_2 & \Phi_2 \\ \overline{W}_4 & V_4 & \Psi_4 & \Phi_4 \\ \overline{W}_5 & V_5 & \Psi_5 & \Phi_5 \end{vmatrix},$$
$$\Delta_{21} = \begin{vmatrix} U_1 & W_1 & \Psi_1 & \Phi_1 \\ U_2 & W_2 & \Psi_2 & \Phi_2 \\ U_4 & W_4 & \Psi_4 & \Phi_4 \\ U_5 & W_5 & \Psi_5 & \Phi_5 \end{vmatrix}, \quad \Delta_{22} = \begin{vmatrix} U_1 & \overline{W}_1 & \Psi_1 & \Phi_1 \\ U_2 & \overline{W}_2 & \Psi_2 & \Phi_2 \\ U_4 & \overline{W}_4 & \Psi_4 & \Phi_4 \\ U_5 & \overline{W}_3 & \Psi_5 & \Phi_5 \end{vmatrix}, \quad \Delta_{41} = \begin{vmatrix} U_1 & V_1 & W_1 & \Phi_1 \\ U_2 & V_2 & W_2 & \Phi_2 \\ U_4 & V_4 & W_4 & \Phi_4 \\ U_5 & V_5 & W_5 & \Phi_5 \end{vmatrix},$$
$$\Delta_{42} = \begin{vmatrix} U_1 & V_1 & \overline{W}_1 & \Phi_1 \\ U_2 & V_2 & \overline{W}_2 & \Phi_2 \\ U_4 & V_4 & \overline{W}_4 & \Phi_4 \\ U_5 & V_5 & \overline{W}_5 & \Phi_5 \end{vmatrix}, \quad \Delta_{51} = \begin{vmatrix} U_1 & V_1 & \Psi_1 & W_1 \\ U_2 & V_2 & \Psi_2 & W_2 \\ U_4 & V_4 & \Psi_4 & W_4 \\ U_5 & V_5 & \Psi_5 & W_5 \end{vmatrix}, \quad \Delta_{52} = \begin{vmatrix} U_1 & V_1 & \Psi_1 & \overline{W}_1 \\ U_2 & V_2 & \Psi_2 & \overline{W}_2 \\ U_4 & V_4 & \Psi_4 & \overline{W}_4 \\ U_5 & V_5 & \Psi_5 & \overline{W}_5 \end{vmatrix}.$$

Appendix C

$$k_1 = (k_{22}L_3 + k_{24}L_5 + k_{25}L_7 + k_{12}L_1 + k_{23})L_3 + (k_{44}L_5 + k_{14}L_1 + k_{34} + k_{45}L_7)L_5 + (k_{11}L_1 + k_{15}L_7 + k_{13})L_1 + k_{33} + (k_{55}L_7 + k_{35})L_7,$$
$$k_2 = (k_{24}L_6 + k_{12}L_2 + k_{25}L_8 + 2k_{22}L_4)L_3 + (k_{24}L_5 + k_{25}L_7 + k_{12}L_1 + k_{23})L_4 + (k_{45}L_8 + k_{14}L_2 + 2k_{44}L_6)L_5 + (k_{13} + k_{15}L_7 + 2k_{11}L_1)L_2 + (k_{14}L_1 + k_{34} + k_{45}L_7)L_6 + (2k_{55}L_7 + k_{15}L_1 + k_{35})L_8,$$
$$k_3 = (k_{22}L_4 + k_{24}L_6 + k_{12}L_2 + k_{25}L_8)L_4 + (k_{11}L_2 + k_{14}L_6 + k_{15}L_8)L_2 + (k_{45}L_6 + k_{55}L_8)L_8 + k_{44}L_6^2 + \mu_3 e_7,$$
$$k_4 = I_1(L_1^2 e_{12} + L_3^2 e_6) + I_7\gamma^2(e_6 + e_{12}) + I_3^*(L_5^2 e_6 + L_7^2 e_{12}) + 2I_2^* e_5(L_1L_5 + L_3L_7) + 2\gamma I_5^*(L_5 e_6 + L_7 e_{12}) + 2I_4\gamma(L_3 + L_1), \quad I_2^* = I_2 + \gamma I_4,$$
$$k_5 = 2I_1(L_1L_2e_{12} + L_3L_4e_6) + 2I_3^*(L_5L_6e_6 + L_7L_8e_{12}) + 2\gamma I_4 e_5(L_2 + L_1L_6 + L_4) + 2\gamma I_5^*(L_8e_{12} + L_6e_6) + 2I_2^* e_5(L_2L_5 + L_4L_7 + L_3L_8), \quad I_3^* = I_7\gamma^2 + 2I_5\gamma + I_3,$$
$$k_6 = I_1(L_4^2 e_6 + L_2^2 e_{12}) + I_3^*(L_8^2 e_{12} + L_6^2 e_6) + 2I_2^* e_5(L_4L_8 + L_2L_6), \quad I_5^* = I_7\gamma^2 + I_5\gamma,$$
$$k_{11} = \tfrac{1}{2}(A_{11}e_{18} + 2A_{16}e_{10} + A_{66}e_{19}), \quad k_{12} = A_{16}e_3 + A_{66}e_{14} + A_{12}e_{18} + A_{26}e_{10},$$
$$k_{13} = e_3 s_{11} + (s_{12} + 2s_{66})e_{10} + (e_{14} + 2e_{18})s_{16} + e_{19}s_{26} + \overline{R}_1 e_5 + \overline{R}_3 e_{16},$$
$$k_{14} = e_3\overline{s}_{11} + (e_{14} + e_{18})\overline{s}_{16} + e_{10}\overline{s}_{66}, \quad k_{15} = e_{10}(\overline{s}_{12} + \overline{s}_{66}) + e_{18}\overline{s}_{16} + e_{19}\overline{s}_{26},$$
$$k_{22} = A_{26}e_3 + \tfrac{1}{2}(A_{22}e_{18} + A_{66}e_{20}), \quad k_{45} = e_{14}\eta_{12}^* + e_3\eta_{16}^* + e_{10}\eta_{26}^* + e_{18}\eta_{66}^* + e_5\zeta_{45},$$
$$k_{23} = e_{10}s_{22} + e_3(s_{12} + 2s_{66}) + (e_{14} + 2e_{18})s_{26} + e_{20}s_{16} + \overline{R}_2 e_5 + \overline{R}_3 e_{13},$$
$$k_{24} = e_3(\overline{s}_{12} + \overline{s}_{66}) + e_{20}\overline{s}_{16} + e_{18}\overline{s}_{26}, \quad k_{25} = e_{10}\overline{s}_{22} + (e_{14} + e_{18})\overline{s}_{26} + e_3\overline{s}_{66},$$
$$k_{33} = 2(e_3\eta_{16} + e_{10}\eta_{26} + e_{18}\eta_{66}) + \tfrac{1}{2}(e_{20}\eta_{11} + 2e_{14}\eta_{12} + e_{19}\eta_{22} + e_{12}\zeta_{44} + 2e_5\zeta_{45} + e_6\zeta_{55}) + \overline{R}_4 e_{13} + \overline{R}_5 e_{16} + \tfrac{1}{2}\overline{R}_7 e_7 + 2\overline{R}_6 e_5,$$
$$k_{34} = e_{20}\overline{\eta}_{11} + e_{14}\overline{\eta}_{12} + 3e_3\overline{\eta}_{16} + e_{10}\overline{\eta}_{26} + 2e_{18}\overline{\eta}_{66} + e_5(\zeta_{45} + \overline{R}_{10}) + e_6\zeta_{55} + e_{13}\overline{R}_8,$$
$$k_{35} = e_{19}\overline{\eta}_{22} + e_{14}\overline{\eta}_{12} + e_3\overline{\eta}_{16} + 3e_{10}\overline{\eta}_{26} + 2e_{18}\overline{\eta}_{66} + e_{12}\zeta_{44} + e_5(\zeta_{45} + \overline{R}_{10}) + \overline{R}_9 e_{16},$$
$$k_{44} = \tfrac{1}{2}(e_{20}\eta_{11}^* + 2e_3\eta_{16}^* + e_{18}\eta_{66}^* + e_6\zeta_{55}), \quad k_{55} = \tfrac{1}{2}(e_{19}\eta_{22}^* + 2e_{10}\eta_{26}^* + e_{18}\eta_{66}^* + e_{12}\zeta_{44}),$$

$$L_1 = -\omega^2\Delta_{11}, \quad L_2 = l\Delta_{11} + \Delta_{12}, \quad L_3 = -\omega^2\Delta_{21}, \quad L_4 = l\Delta_{21} + \Delta_{22},$$
$$L_5 = -\omega^2\Delta_{41}, \quad L_6 = l\Delta_{41} + \Delta_{42}, \quad L_7 = -\omega^2\Delta_{51}, \quad L_8 = l\Delta_{51} + \Delta_{52},$$

$$a_1 = -4k_6l^6, \quad a_2 = 4k_6l^4(l + 2k_3^3\omega^2), \quad a_3 = k_2k_6l^2(k_2l^2 + 4k_3\omega^2l + 4k_3^2\omega^4),$$
$$a_4 = -4k_3^3(2k_3\omega^2 + k_2l), \quad a_6 = -2k_1, \quad a_5 = k_3^3(4k_3k_1 - k_2^2), \quad a_7 = -4k_3k_6l^4,$$
$$a_8 = 21(k_3^2k_5l^3 - k_2k_3k_6l^3 - k_3^3l^2), \quad a_9 = 2k_3^2k_6l^2, \quad a_{10} = 2k_3^2(2k_3^2 - k_3l + k_6l),$$
$$a_{11} = \tfrac{1}{2}k_3(4k_3^3k_4 + k_2^2k_6 - 2k_2k_3^2k_5), \quad a_{12} = 4k_3^4, \quad a_{13} = 2k_6l^5(k_2 + 2k_3l\omega^2),$$
$$a_{14} = -a_1, \quad a_{15} = k_3^2a_7, \quad a_{16} = 2k_3^2l^2(k_5l - 2k_2k_6l - 2k_6\omega^2 - 2k_3),$$
$$a_{17} = e_2k_3^2k_5l^2 + 2k_3^3k_5l\omega^2 - k_2^2k_3k_6l^2 - 2k_2k_3^2l\omega^2k_6 - 4k_3^4\omega^2 - 2k_2k_3^3l.$$

References

[1] O'Donoghue PE, Atluri SN. Control of dynamic response of a continuum model of a large space structure. Comput Struct 1986;23:199–209.
[2] Turvey GJ, Marshall IH. Buckling and postbuckling of composite plates. Chapman & Hall; 1995.
[3] Rao SS. Optimum design of structures under shock and vibration environment. Shock Vib Digit 1989;21:3–15.
[4] Yang JN, Soong TT. Recent advances in active control of civil engineering structures. Probab Engng Mech 1988;3:179–88.
[5] Miller RK, Masri SF, Dehganyer TJ, Caughey TK. Active vibration control of large civil structures. ASCE J Engng Mech 1988;114:1542–70.
[6] Adali S, Richter A, Verijenko VE. Minimum weight design of symmetric angle-ply laminates with incomplete information on initial imperfections. J Appl Mech 1997;64:90–6.
[7] Adali S, Sadek IS, Sloss JM, Bruch Jr JC. Distributed control of layered orthotropic plates with damping. Optimal Control Appl Methods 1988;9:1–17.
[8] Muc A, Krawiec Z. Design of composite plates under cyclic loading. Compos Struct 2000;48(1–3):139–44.
[9] Bruch JC, Adali S, Sloss JM, Sadek IS. Optimal design and control of cross-ply laminate for maximum frequency and minimum dynamic response. Comput Struct 1990;37:87–94.
[10] Langthjem MA, Sugiyama Y. Optimum design of cantilevered columns under the combined of conservative and nonconservative loads. Part II: The damped case. Comput Struct 2000;74:399–408.
[11] Walker M. Optimal design of symmetric laminates with cut-outs for maximum buckling load. Comput Struct 1999;70:337–43.
[12] Sussmann HJ, Willems JC. 300 years of optimal control: from the brachystochrone to the maximum principle. IEEE Control Syst 1997:32–44.
[13] Duvaut G, Terrel G, Léné F, Verijenko VE. Optimization of fiber reinforced composites. Compos Struct 2000;48(1–3):83–9.
[14] Ledzewicz U. Extension of the local maximum principle control problem. J Optim Theory Appl 1993;77(3):661–80.
[15] Fares ME, Zenkour AM. Buckling and free vibration of non-homogeneous composite cross-ply laminated plates with various plate theories. Compos Struct 1999;44:279–87.
[16] Reddy JN. Mechanics of composite materials and structures. Theory and analysis. Florida: CRC Press; 1997.
[17] Zenkour AM, Fares ME. Thermal bending analysis of composite laminated cylindrical shells using a refined first-order theory. J Therm Stresses 2000;23:505–26.
[18] Fares ME, Youssif YG, Alamir AE. Optimal design and control of composite laminated plates with various boundary conditions using various plate theories. Compos Struct 2002;56:1–12.
[19] Youssif YG, Fares ME, Hafiz MA. Optimal control of the dynamic response of anisotropic plate with Various Boundary Conditions. Mech Res Commun 2002;28(5):525–34.
[20] Reddy JN, Liu CF. A higher-order shear deformation theory of laminated elastic shell. Int J Engng 1985;23(3):319–30.
[21] Letov AM. Analytical design of controllers. Aftamateka and Telemchanika 1960;21(4–6), 1961;22 (4).
[22] Gabralyan MS. About stabilization of mechanical systems under continuous forces, YGU. Yervan 1975;2:47–56.